Reversible hydrogen storage behaviors and microstructure of TiC-doped sodium aluminum hydride

Xiulin Fan · Xuezhang Xiao · Jiechang Hou ·
Zheng Zhang · Yuanbo Liu · Zhe Wu ·
Changpin Chen · Qidong Wang · Lixin Chen

Abstract TiC-doped $NaAlH_4$ complex hydride was prepared by hydrogenating of ball-milled NaH/Al mixture in the presence of 5 mol% TiC powder, and its hydrogen storage behaviors and microstructure were investigated. It is found that TiC is a good catalyst for the reversible hydriding/dehydriding process of $NaAlH_4$ at moderate temperatures by reducing the decomposition temperature and improving the hydriding/dehydriding kinetics. The hydrogen desorption capacity of 5 mol% TiC-doped $NaAlH_4$ is 4.6 wt% at 165 °C and its average dehydriding rate in the first 30 min reaches 0.107 wt%/min. X-ray diffraction analyses show that the size of crystal grains of the composites is reduced by ball-milling, and is then increased rapidly in the first hydriding–dehydriding cycle. Scanning electron micrographs represent that the particle size of the ball-milled composites is quite even and averages around 50 nm. However, it changes into a widely distributed one ranging from 50 nm to 1 μm in the subsequent hydriding–dehydriding cycles. DSC measurement indicates that the doping of TiC can lower the dehydriding temperatures of sodium aluminum hydride.

Introduction

Hydrogen, which is mutually convertible with all renewable energies and burns into water in air, is regarded as the most ideal energy vector in near future. Yet, there are still a few hard technical problems confronting us. One of the main problems to be solved is the storage of hydrogen. Traditional metal hydrides such as $LaNi_5H_6$ and $TiMn_{1.5}H_{2.47}$ store hydrogen reversibly and safely for practical usage, but their hydrogen storage capacities are too low (less than 2.5 wt%). In 1997, Bogdanovic et al. [1] demonstrated that the dehydrogenation and rehydrogenation are possible for sodium alanate ($NaAlH_4$) by using titanium-based compounds as catalysts. This finding offers a clear potential to achieve high hydrogen capacity at a moderate temperature, thus quickly stimulates extensive research interests in developing catalytically enhanced sodium alanate [2–10].

It is well-known that $NaAlH_4$ releases a theoretical hydrogen capacity of 5.6 wt% via a two-step reaction as:

$$3\ NaAlH_4 \ \leftrightarrow Na_3AlH_6 + 2Al + 3H_2$$
$$\leftrightarrow 3NaH + 3Al + 4.5H_2 \quad (1)$$
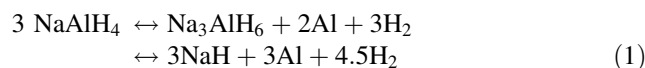
It was known that $NaAlH_4$ catalyzed with Ti and/or other transition metals by dry ball-milling enabled the reversible hydrogen desorption/absorption reactions to take place under milder conditions [1–11]. The addition of a small amount of Ti halides such as $TiCl_3$, $TiCl_4$ and TiF_3 to $NaAlH_4$ during ball-milling is currently widely used as a method for catalyzing $NaAlH_4$. Although Ti halides significantly improve the dehydriding/rehydriding kinetics of $NaAlH_4$, their addition reduces the hydrogen capacity of $NaAlH_4$ due to the formation of Na halides as the reaction byproducts between NaH and/or $NaAlH_4$ with Ti halides [12–15]. Therefore, there have been persistent efforts to find new effective catalysts that enhance the reaction kinetics while maintaining the high hydrogen capacity. Bogdanovic et al. [16] doped TiN nanoparticles to $NaAlH_4$, and achieved hydrogen capacity of about 5.0 wt% within 17 cycles. However, this catalyst is quite complicated to prepare. Lee et al. [17] catalyzed Li_3AlH_6 with Ti_5Si_3 which was proved effective in releasing more hydrogen from Li_3AlH_6 than Ti

X. Fan · X. Xiao · J. Hou · Z. Zhang · Y. Liu · Z. Wu ·
C. Chen · Q. Wang · L. Chen (✉)
Department of Materials Science and Engineering, Zhejiang
University, Hangzhou 310027, People's Republic of China
e-mail: lxchen@zju.edu.cn

halides, yet the hydriding/dehydriding kinetics became not satisfactory. Suttisawat et al. [18] investigated the TiO_2-doped $NaAlH_4$, and got a reversible hydrogen capacity of about 3.5 wt%. In light of those studies, we started as well to find some other titanium compounds capable of stimulating the hydriding/dehydriding kinetics of sodium alanate and maintaining meanwhile their high hydrogen storage capacities. It was reported that TiC was catalysis for hydrogenation reactions of some chemical products [19, 20]. Moreover, the molecular weight of TiC is much lower than those of $TiCl_3$ and TiO_2. So, if the same mole percent additives are doped into the sodium alanate, $NaAlH_4$ doped with TiC will exhibit a higher theoretical hydrogen storage capacity. Thus, in the present study, we chose TiC as the dopant, prepared a NaH/Al composite and doped the composite with 5 mol% TiC powder by dry ball-milling, and finally hydrogenated the composite to get the TiC-doped $NaAlH_4$ sample. The hydrogen storage behaviors and microstructure of TiC-doped $NaAlH_4$ were then systematically investigated.

Experimental

The starting materials were NaH powder (95%, 74 μm, purchased from Sigma-Aldrich Corp.), Al powder (99%, 74–154 μm), TiC powder (99%, <4 μm, obtained from Sigma-Aldrich Corp.), all being used as-received. The powder mixtures of NaH + Al + TiC in a molar ratio of 1:1:0.05 were mechanically milled for 48 h by a planetary mill at 300 rpm. The milling was performed under a hydrogen atmosphere with initial pressure of 0.6 MPa. The ball to powder weight ratio is 30:1. In a parallel investigation for comparing, the powder mixtures without TiC were prepared in the same way. All operations on specimens were performed in an Ar-filled glove box with the H_2O and O_2 levels <1 ppm.

The hydriding/dehydriding processes of the samples were carried out on a carefully calibrated Sievert's type apparatus. The hydrogenation process was carried out at 120 °C under the initial hydrogen pressure of 12 MPa, while the dehydrogenation was proceeded at the temperature from 150 to 165 °C against 0.1 MPa. Before hydriding, samples were heated each time to 170 °C under vacuum for 1 h. To minimize the H_2O/O_2 contamination, supra pure hydrogen gas (99.9999%) was adopted. Hydrogen capacities were calculated on the basis of the total weight of the samples including the weight of catalyst.

The crystal structures of as-prepared materials were characterized with powder X-ray diffraction (XRD, ARL-X'TRA with Cu-K$_\alpha$ radiation, Thermo Electron Corp.). For minimizing the H_2O/O_2 contamination during XRD examination, a thin layer of a special plastic tape which has

a negligible effect on diffraction patterns was used to cover the surface of the samples. The surface morphology of the samples was studied with a scanning electron microscope (SEM, Hitachi S-4800). Differential scanning calorimetry (DSC) measurements were carried out on a Netzsch DSC 200F3 at the heating rate of 5 °C/min from 50 to 300 °C.

Results and discussion

The X-ray diffraction patterns of the ball-milled NaH/Al + 5 mol% TiC composite in different hydrogenation and dehydrogenation stages are shown in Fig. 1. It can be seen that the ball-milled sample before first hydrogenation contains some small amount of Na_3AlH_6, while Al and NaH are the main phases. Moreover, it should be pointed out that the diffraction peaks of the sample before the first hydrogenation are broader than those of the sample after hydrogenation and dehydrogenation. This represents that the crystal grains of the sample before the first hydrogenation are finer compared with those in the sample after hydrogenation and dehydrogenation. After hydrogenation, the main phase of the sample turns to $NaAlH_4$, however, there are still a few Na_3AlH_6 and Al phases left unreacted. In the XRD pattern of the sample after being dehydrided for 10 h, the $NaAlH_4$ phase disappears, while residual Na_3AlH_6 is observed, suggesting that the hydrogenation reaction is not fully completed. As TiC powder is thermodynamically more stable than alkali hydride in the process of milling/hydriding/dehydriding, it is kept intact in the milling/hydriding/dehydriding processes as shown in Fig. 1, so it does not produce the "dead weight" of byproduct such as Na halide, and the sodium alanate
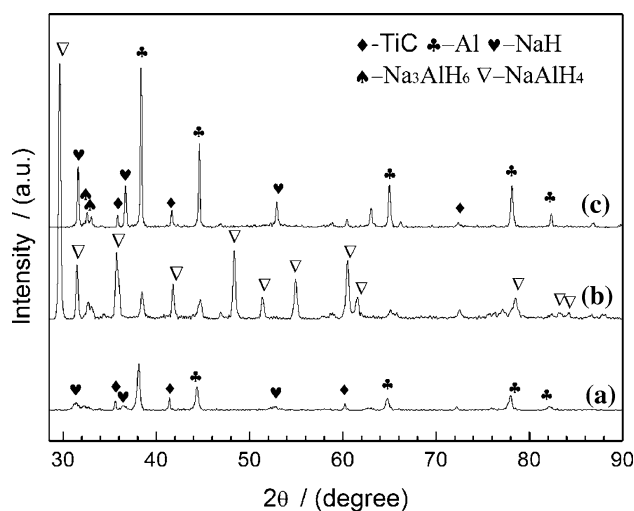

Fig. 1 XRD patterns of the ball-milled NaH/Al composite doped with 5 mol% TiC: (a) before first hydrogenation; (b) after first hydrogenation at 120 °C; (c) after first dehydrogenation at 155 °C

system can maintain relatively high hydrogen storage capacity. This also indicates that the reversible hydrogen storage process of TiC-doped NaAlH$_4$ may be governed by a heterogeneous surface catalysis mechanism [9].

Due to the high affinity of sodium aluminum hydrides to oxygen/moisture, it is very difficult to measure and define the average particle size of the samples by Particle Size Analyzers. So, SEM was extensively used to examine the particle size and surface morphology of sodium alanate samples [21–25]. Figure 2 shows SEM micrographs of the NaH/Al composite doped with 5 mol% TiC before the first hydrogenation and after the first dehydrogenation at 155 °C. It is found that the particle of the ball-milled composite is quite even at about 50 nm in size before the first hydrogenation. However, a lot of composite particles aggregate and grow up in the process of the first hydrogenation, and the particle size of the composite exhibits a wide particle size distribution ranging from 50 nm to 1 μm after the first hydrogenation and dehydrogenation. With the help of SEM, it is difficult to determine and define the average size, so here we just present the particle size distribution range of the composite samples.
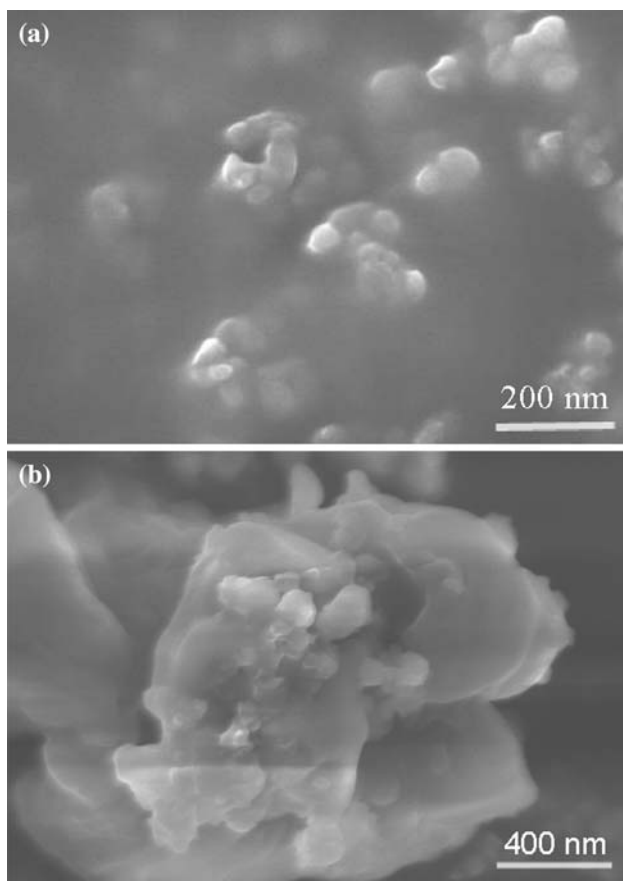

Fig. 2 SEM micrographs of the ball-milled NaH/Al composite doped with 5 mol% TiC: **a** before first hydrogenation; **b** after the first dehydrogenation at 155 °C
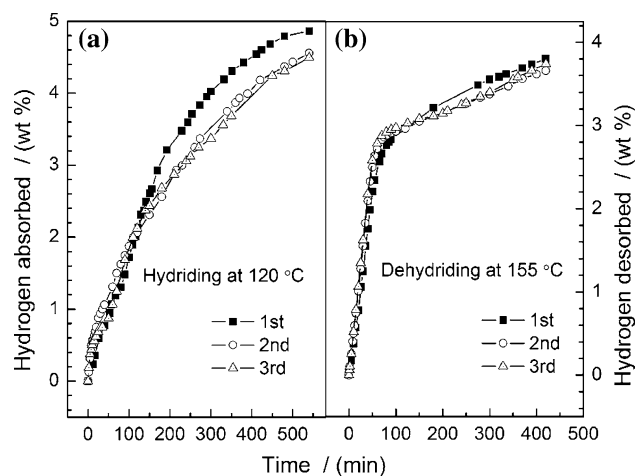

Fig. 3 Hydriding/dehydriding curves of the NaH/Al composite doped with 5 mol% TiC: **a** hydriding at 120 °C under 12 MPa hydrogen pressure; **b** dehydriding at 155 °C against 0.1 MPa

The hydriding curves of 5 mol% TiC-doped NaH/Al composite at 120 °C under 12 MPa hydrogen pressure are shown in Fig. 3a. It can be seen that the composite has the highest hydrogen absorption capacity of 4.86 wt% and the hydriding rate for the first hydrogenation process is the fasted one. However, the hydriding rates in the subsequent cycles are slowing down, and the hydrogen absorption capacities within 540 min in the second cycle and third cycle are very close to 4.50 wt%, both are deteriorated compared with that in the first cycle. We believe that this phenomenon is related to the size change of the composite particles and crystal grains of the sample. It is well-known that the bulk diffusion of Al in the alanate is the rate-limiting step in the dehydrogenation of Ti-doped NaAlH$_4$ [26]. When the particle size is decreased to nanometer range, the hydriding/dehydriding kinetics can be improved greatly [27–29]. This explains why the hydriding rate and hydrogen absorption capacity in the first cycle are the highest. From the hydriding curves, it can also be seen that, before the amounts of hydrogen absorbed reaches about 2.1 wt%, the difference of the hydriding rates in different cycle is very small, however, the difference enlarges quickly after hydrogen absorbed exceeds 2.1 wt%. It means that the second step of hydrogenation reaction is more sensitively affected than the first step due to the growth in particle sizes and crystal grains. Figure 3b shows the dehydriding curves of the hydrogenated sample at 155 °C against 0.1 MPa. It is found that there is little difference amongst the dehydriding behaviors in different cycles. The hydrogen desorption capacities within 420 min in the first three cycles are all about 3.8 wt%, with the hydrogen desorption capacity in the first cycle slightly higher than the other two. As mentioned hereinbefore, the particle size of the composite become much bigger after

the first hydrogenation, and has little change in the following dehydriding/rehydriding cycles. This makes us believe that particle size is an important factor on the hydrogenation behaviors in the first cycle and subsequent cycles.

In the present study, the size effect of the composite particles is displayed by the difference in hydrogen absorbed between the first hydrogenation behavior and the following ones. However, after the first hydrogenation, the particle size has become bigger and invariable, so we believe that the size effect is finite.

In order to approve the improvement effect of TiC on the hydrogenation and dehydrogenation process of sodium alanate, a comparison experiment was carried out. A comparison of the hydrogen absorption/desorption in the second cycle between the sample doped with 5 mol% and the undoped sample is shown in Fig. 4. It can be clearly seen that, the undoped sample absorbs very little hydrogen hardly reaching 0.43 wt% in 9 h, however, the sample doped with 5 mol% TiC displays a remarkable improvement in the hydriding kinetics of the composite. For hydrogen desorption, the catalytic effect of TiC is also impressive. Furthermore, as TiC does not react with the reactants (NaH, Al, and $NaAlH_4$) and remains stable throughout the entire cycling process. It will not produce other Ti-containing phases which may act as the active species. So TiC may serve as a surface catalyst enhancing the hydriding/dehydriding reactions during the hydrogenation and dehydrogenation process.

The effect of dehydriding temperature on the dehydriding properties of TiC-doped $NaAlH_4$ has also been investigated, as shown Fig. 5. The vertical dashed line drawn in Fig. 5 is to acquire data for calculating the dehydriding rate at the initial dehydriding period of 30 min. The hydrogen desorption capacity at 480 min and initial dehydriding rate (namely the rate of the first 30 min) are presented in the
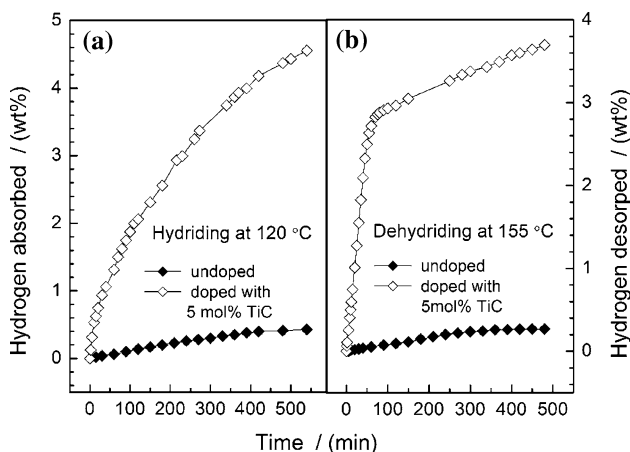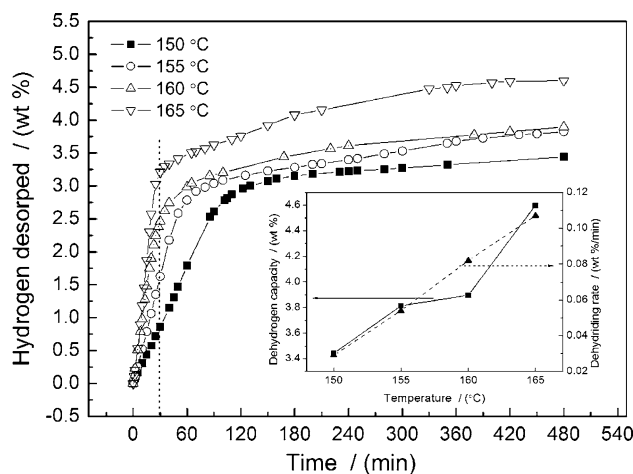

Fig. 5 Dehydriding curves of hydrided NaH/Al composite doped with 5 mol% TiC at different dehydriding temperatures. The inset is the hydrogen desorption capacities and initial dehydriding rates (measured in the first 30 min)

inset. The composites were first hydrided at 120 °C under 12 MPa for 12 h before dehydrogenation. For making the results comparable, the data shown are all collected for the second dehydriding cycle. It can be seen clearly that the dehydriding characteristics are highly temperature dependent, which is very similar to that of $NaAlH_4$ doped with $Ti(OBu)_4$ or Ti [30, 31]. As the dehydriding temperature rises, both the hydrogen desorption capacity in 8 h and the dehydriding rate increase quickly. When the temperature rises up to 165 °C, the hydrogen desorption capacity and initial dehydriding rate of the first 30 min reach 4.60 wt% and 0.107 wt%/min, respectively.

Figure 6 represents the DSC curves of undoped $NaAlH_4$ and hydrided NaH/Al composite doped with 5 mol% TiC. The two distinct endothermic peaks of the DSC curves correspond to the two hydrogen desorption steps in Eq. 1.
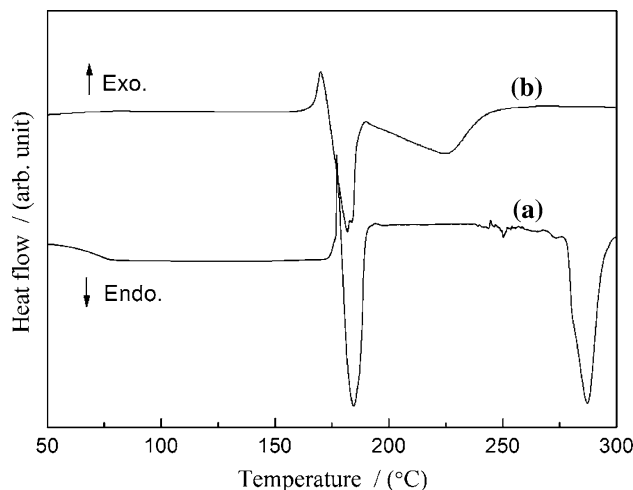

Fig. 4 Hydriding/dehydriding curves of the 5 mol% TiC-doped and undoped NaH/Al composites in the second cycle

Fig. 6 DSC curves of undoped $NaAlH_4$ (a) and hydrided NaH/Al composite doped with 5 mol% TiC (b)

It is found that the two endothermic peaks of the hydrided NaH/Al composite doped with TiC both shift to lower temperatures, especially for the second step reaction. $NaAlH_4$ without catalyst starts to decompose and release H_2 gas at about 180 °C and the peak temperature is about 185 °C. On the other hand, the decomposition of hydrided NaH/Al composites doped with 5 mol% TiC starts at about 170 °C and with its the peak at about 182 °C. When it comes to the second step decomposition, the difference becomes more notable. The TiC-doped composite starts to decompose at about 190 °C, while the undoped composite does not decompose until 275 °C. These decreases in decomposition temperatures are similar to those of $NaAlH_4$ using Ti as catalyst in previous investigations [32, 33]. This experiment shows that the dopant TiC lowers the dehydrogenation temperatures of $NaAlH_4$ and Na_3AlH_6 clearly. As DSC scans at a definite heating rate, the actual equilibrium temperatures for the reactions should be somewhat below the temperatures reported. From the DSC curves, we also can see that the second endothermic peak of the hydrided NaH/Al composites doped with TiC becomes much broader than the first one, which is consistent with the poorer kinetics of the second decomposition reaction.

Conclusions

TiC is proved to have a good catalytic effect on the reversible hydriding/dehydriding behaviors of $NaAlH_4$ at moderate temperatures. TiC does not react with the reactants (NaH, Al, and $NaAlH_4$) and remains stable throughout the whole process of milling/hydriding/dehydriding. It is found that the particles and crystal grains of the composites are reduced in size by ball-milling, and then grow up rapidly in the first hydrogenation process. This rapid grain growth brings about the marked difference in hydriding behavior between the first cycling process and the second/third ones. The dehydriding characteristics of TiC-doped $NaAlH_4$ are highly temperature dependent. As the dehydriding temperature rises, both the hydrogen desorption capacity and the dehydriding rate increase quickly. The hydrogen desorption capacity of 5 mol% TiC-doped $NaAlH_4$ reaches 4.6 wt% at 165 °C within 8 h. DSC measurements also show that 5 mol% TiC added as catalyst lowers markedly the dehydriding temperatures of $NaAlH_4$ and Na_3AlH_6.

References

1. Bogdanović B, Schwickardi M (1997) J Alloys Compd 253–254:1
2. Zidan RA, Takara S, Hee AG, Jensen CM (1999) J Alloys Compd 285:119
3. Zaluska A, Zaluski L, Ström-Olsen JO (2000) J Alloys Compd 298:125
4. Gross KJ, Thomas GJ, Jensen CM (2002) J Alloys Compd 330–332:683
5. Anton DL (2003) J Alloys Compd 356–357:400
6. Sun DL, Srinivasan SS, Chen GR, Jensen CM (2004) J Alloys Compd 373:265
7. Wang P, Jensen CM (2004) J Phys Chem B 108:15827
8. Bogdanović B, Felderhoff M, Pommerin A, Schuth F, Spielkamp N (2005) Adv Mater 18:1198
9. Kang XD, Wang P, Cheng HM (2007) Int J Hydrogen Energy 32:2943
10. Suttisawat Y, Rangsunvigit P, Kitiyanan B, Muangsin N, Kulprathipanja S (2007) Int J Hydrogen Energy 32:1277
11. Weidenthaler C, Pommerin A, Felderhoff M, Bogdanović B, Schüth F (2003) Phys Chem Chem Phys 5:5149
12. Sandrock G, Gross K, Thomas G (2002) J Alloys Compd 339:299
13. Majzoub EH, Gross KJ (2003) J Alloys Compd 356–357:363
14. Brinks HW, Jensen CM, Srinivasan SS, Hauback BC, Blanchard D, Murphy K (2004) J Alloys Compd 376:215
15. Haiduc AG, Stil HA, Schwarz MA, Paulus P, Geerlings JJC (2005) J Alloys Compd 393:252
16. Bogdanović B, Felderhoff M, Kaskel S, Pommerin A, Schlichte K, Schüth F (2003) Adv Mater 15:1012
17. Lee GJ, Shim JH, Cho YW (2007) J Mater Sci 42:6302. doi: 10.1007/s10853-006-1173-6
18. Suttisawat Y, Jannatisin V, Rangsunvigit P, Kitiyanan B, Muangsin N, Kulprathipanja S (2007) J Power Sources 163:997
19. Kojima I, Miyazaki EY, Yasumori I (1979) J Catal 59:472–474
20. Kojima I, Miyazaki E (1984) J Catal 89:168–171
21. Kang XD, Wang P, Cheng HM (2007) J Phys Chem C 111:4879
22. Okada N, Genma R, Nishi Y, Uchida HH (2004) J Mater Sci 39:5503. doi:10.1023/B:JMSC.0000039274.80645.5d
23. Sun T, Zhou B, Wang H, Zhu M (2009) J Alloys Compd 467:413
24. Thomas GJ, Gross KJ, Yang NYC, Jensen C (2002) J Alloys Compd 330–332:702
25. Wang J, Ebner AD, Prozorov T, Zidan R, Ritter JA (2005) J Alloys Compd 395:252
26. Gunaydin H, Houk KN, Ozolins V (2008) Proc Natl Acad Sci USA 105:3673
27. Balde CP, Hereijgers BPC, Bitter JH, Jong KP (2006) Angew Chem Int Ed 45:3501
28. Zheng SY, Fang F, Zhou GY, Chen GR, Ouyang LZ, Zhu M, Sun DL (2008) Chem Mater 20:3954
29. Baldé CP, Hereijgers BPC, Bitter JH, Jong KP (2008) J Am Chem Soc 130:6761
30. Bogdanović B, Brand RA, Marjanovic A, Schwickardi M, Tolle J (2000) J Alloys Compd 302:36
31. Xiao XZ, Chen LX, Wang XH, Li SQ, Wang QD, Chen CP (2007) Int J Hydrogen Energy 32:3954
32. Xiao XZ, Chen LX, Wang XH, Li SQ, Wang QD, Chen CP (2008) Int J Hydrogen Energy 33:64
33. Xiao XZ, Chen LX, Fan XL, Wang XH, Chen CP, Lei YQ, Wang QD (2009) Appl Phys Lett 94:041907